Science of the Total Environment 670 (2019) 779–788

Contents lists available at ScienceDirect

Science of the Total Environment

journal homepage: www.elsevier.com/locate/scitotenv

Prussian blue immobilized cellulosic filter for the removal of aqueous cesium

Hyowon Kim [a], Hyobin Wi [b], Sungwon Kang [c], Sunho Yoon [d], Sungjun Bae [d], Yuhoon Hwang [a,*]

[a] Department of Environmental Engineering, Seoul National University of Science and Technology, 232 Gongneung-ro, Nowon-gu, Seoul 01811, Republic of Korea
[b] Department of Materials and Environmental Engineering, Seoul National University, 1 Gwanak-ro, Gwanak-gu, Seoul 08826, Republic of Korea
[c] Department of Land, Water and Environment Research, Korea Institute of Civil Engineering and Building Technology, 283 Goyang-daero, Ilsanseo-gu, Goyang-si, Gyeonggi-do 10223, Republic of Korea
[d] Department of Civil and Environmental Engineering, Konkuk University, 120 Neungdong-ro, Gwangjin-gu, Seoul 05029, Republic of Korea

HIGHLIGHTS

- PB was immobilized on a cellulose filter for selective cesium adsorption.
- The AA functionalization contributed to stable PB formation and reduced PB leaching.
- CF-AA-PB showed 16.66 mg/g of cesium adsorption capacity.
- Effect of water matrix was not severe indicating selective adsorption ability.
- The CF-AA-PB can be effectively used as filter material for water intake.

GRAPHICAL ABSTRACT

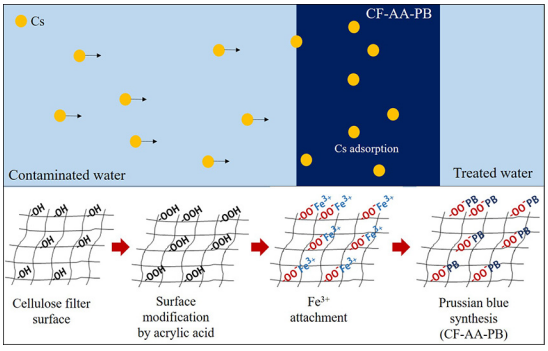

ARTICLE INFO

Article history:
Received 23 December 2018
Received in revised form 26 February 2019
Accepted 15 March 2019
Available online 18 March 2019

Editor: Bingcai Pan

Keywords:
Nuclear accident
Cesium
Prussian blue
Cellulose filter
Immobilization
Adsorption

ABSTRACT

Cesium is a typical radioisotope that has a long half-life and is dangerous and can be emitted in the event of a nuclear accident. Prussian blue (PB), which is known to effectively adsorb cesium, is difficult to separate when it is dissolved in an aqueous system. In this study, PB was immobilized on a filter type support media, cellulose filter (CF), for use as a selective material for cesium adsorption. The commercially available CF was functionalized by the addition of acrylic acid (AA) (i.e., CF-AA) to enhance the PB immobilization, which increased both PB loading and binding strength. The AA functionalization changed the major functional groups from hydroxyl to carboxylic, as confirmed by Fourier-transform infrared spectroscopy. As a result of the surface modification, the PB immobilization increased 1.5 times and reduced detachment of PB during washing. The prepared adsorbent, CF-AA-PB, was tested for its cesium adsorption capability. Cesium adsorption equilibrated within 3 h, and the maximum cesium adsorption capacity was 16.66 mg/g. The observed decrease in the solution pH during cesium adsorption inhibited the overall cesium uptake; however, this was minimized by buffering. The prepared CF-AA-PB was used as a filter material and its potential use as a countermeasure for removing radioactive cesium from a contaminated water stream was demonstrated.

* Corresponding author.
E-mail address: yhhwang@seoultech.ac.kr (Y. Hwang).

https://doi.org/10.1016/j.scitotenv.2019.03.234
0048-9697/

1. Introduction

Globally, the increase in energy demand and the exhaustion of fossil fuels are becoming serious problems. Nuclear energy has the advantage of economical and stable supply because of the low cost of energy generation and high energy density (Dresselhaus and Thomas, 2001; Forsberg, 2009). On the basis of these advantages, nuclear energy is used globally, accounting for 10% of the world's electricity as of 2017 (International Atomic Energy Agency, 2018b). As of 2018, 454 nuclear reactors are being operated in the world and 54 additional nuclear reactors are under construction (International Atomic Energy Agency, 2018). Nuclear energy has various advantages, but there is a risk of potentially disastrous nuclear accidents. Among the nuclear power plants operating in the world, 298 old nuclear power plants are more than 30 years old and account for 65.6% of all nuclear power plants (International Atomic Energy Agency, 2018). There were 22 nuclear accidents from 1956 to 2016. The most serious accidents were the Chernobyl nuclear accident in 1986 and the Fukushima nuclear power plant accident in 2011 (International Atomic Energy Agency, 2018c). Nuclear accidents are occurring all over the world, and even if a country does not use nuclear power plant, damage cannot be avoided if an accident occurs in a neighboring country.

Cs^{134} and Cs^{137} among the radioactive materials emitted during a nuclear accident are representative radioisotopes. After the Fukushima nuclear accident in 2011, Cs^{134} and Cs^{137} spread over a large area, and restoration work has been ongoing for several years (Aoyama and Hirose, 2004; Buesseler et al., 2012; Honda et al., 2012; Manolopoulou et al., 2011; Nuclear Regulation Authority Japan, 2018). Compared to other radionuclides, radioactive cesium has a large diffusion coefficient when it enters the water system, and its hydration radius is small, and thus it is easily dissolved in water and very difficult to remove (Awual et al., 2014; Ma et al., 2017). The half-life is longer compared to other radionuclides at 30 years and the biological half-life is 100 days (El-Kamash, 2008; Jia and Wang, 2017). Furthermore, it is chemically similar to sodium and potassium and hence is readily absorbed by living organisms (El-Kamash, 2008). Cesium that is absorbed in the body is not released, causing β-decay, continuous exposure to the body, and cancer and genetic diseases (Jia and Wang, 2017; Olatunji et al., 2015; Sangvanich et al., 2010).

Among the various methods for removing radioactive cesium, adsorption is economical, a relatively simple process, and advantageous in that no additional treatment is required after removal of the target element (Ali et al., 2018; El-Kamash, 2008; Saleh et al., 2016; Tka et al., 2018; Yuan and Smith, 2015; Tan et al., 2018). Prussian blue (PB) is a dark blue dye with the formula $Fe_4[Fe(CN_6)]_3$ and has a constant cubic lattice structure surrounded by cyanide and metal ions as iron ferrocyanide (Ishizaki et al., 2013). It is known that the size of the cubic lattice of PB is well matched with the size of hydrated cesium ions, which are known to effectively remove cesium (Delchet et al., 2012; Haas, 1993; Kong et al., 2014; Loos-Neskovic et al., 2004; Pau et al., 1990). The alkali metal ion adsorption capacity of PB is considered to be $Cs^+ > K^+ > Na^+$. This is because these hydrated ions have dimensions of 3.29 Å, 3.31 Å, and 3.58 Å, respectively, and smaller cesium ion is thus well matched to the PB lattice structure (Alamudy and Cho, 2018; Nightingale, 1959). In the Chernobyl accident, people who were exposed to cesium were given PB pills (Faustino et al., 2008).

However, PB is a very small material with a size of 5–200 nm and is highly dispersible, and hence it is difficult to separate and recover when it enters the water system (Kim et al., 2018b; Yang et al., 2014a). Therefore, it is difficult to apply it directly to water treatment. Accordingly, studies on immobilization of PB on larger supporting materials that can be recovered after use are intensively ongoing. Research to produce filter type adsorbent containing PB (Kim et al., 2018a; Kim et al., 2018b; Qian et al., 2018), composites combining magnetic material and PB to facilitate removal by magnetic force (Yang et al., 2016; Yang et al., 2017), carbon nanomaterials such as CNTs and GO (Basu et al., 2018; Chen et al., 2016; Hu et al., 2012; Kadam et al., 2016), PB containing beads using a polymer material (Kim et al., 2018; Lai et al., 2016; Vipin et al., 2013), PB immobilization on porous material (Turgis et al., 2013), and natural minerals as a PB support (Alamudy and Cho, 2018) has been introduced. The various composite materials with PB showed a superior cesium adsorption capacity with high cesium selectivity, which makes it a suitable material for cesium remediation. However, the complexity of material fabrication should be considered for a practical application.

In the present study, we attempted to enhance the practical applicability to an actual water treatment process by immobilizing PB on a filter material for use as a simple unit process during the water treatment process. Cellulose filter (CF) was selected as supporting material for PB immobilization because it has several advantages including its ready availability in the market, low cost, and high permeability, and that it is easy to produce in the desired size (Roy et al., 2009). Its porous nature allows water to penetrate into the sponge and provides room for PB synthesis. Moreover, this commercial filter material has already proven mechanical strength and stability.

In our previous study (Wi et al., 2019), we developed a protocol to functionalize commercially available supporting materials to immobilize PB and made it stable for contaminated water remediation. In the previous study, poly(acrylic acid) (PAA) was suggested for the surface functionalization of the polyvinyl alcohol (PVA) sponge to convert hydroxyl groups into carboxylic groups for better PB attachment. This phenomenon can be explained by the HSAB theory. Carboxylates are hard Lewis base, therefore, it forms a strong bond with hard Lewis acids including Fe^{3+}. This concept is commonly used in the field of MOF (metal organic framework) research (Yuan et al., 2018). Because acrylic acid (AA) includes a double bond, and carboxylic groups have a negative charge, AA is capable of trading electrons to alkali metals (Smuleac et al., 2010). This approach overcomes the weak bonding of hydroxyl groups in previous studies, and the method can be applied to various supporting materials that contain hydroxyl groups (Yang et al., 2014b; Ge and Wang, 2017).

The cellulose filter has hydroxyl groups on the surface, but ionic bonding between the hydroxyl groups and PB particles is weak compared to other functional groups (carboxylic, amine), and therefore the immobilized PB can be easily eluted into the water. Surface modification of the cellulose filter was therefore carried out in order to modify the major functional group as a carboxyl group to provide stronger binding of PB (Ge and Wang, 2017).

The aim of this work was to develop an approach to produce a PB based composite adsorbent for radioactive cesium uptake. The suggested approach includes using commercial materials as a supporting matrix and functionalizing by a simple chemical reaction to obtain carboxylic groups, and synthesizing PB by layer-by-layer (LBL) assembly. The overall procedures we suggest showed higher loading of PB and stronger stability to prevent leaching of PB in an aqueous solution. Cesium adsorption ability was evaluated through adsorption kinetics and isotherm tests. The effects of pH and the water matrix were also evaluated to determine the adsorption mechanism. Lastly, a continuous filtration test with our PB based filter demonstrated its feasibility for use in a water treatment process to remediate aqueous cesium.

2. Materials and methods

2.1. Materials

The cellulose filter (CF) to be used as support was purchased from Taebong (Korea). Its tensile strength and permeability coefficient were measured as 1.22 N/cm^2 and 0.079 cm/s, respectively. Acrylic acid (AA, 99%), potassium persulfate (KPS, 99%), sodium chloride (NaCl, 93%), and ethanol (99%) were purchased from Samchun Chemical Reagent Corporation Ltd. (Korea) for surface modification. Iron(III) chloride hexahydrate ($FeCl_3 \cdot 6H_2O$, 97%) and potassium ferrocyanide

trihydrate ($K_4[Fe(CN)_6]\cdot 3H_2O$, 99%) as a precursor for PB synthesis were purchased from Duksan Chemical Reagent Corporation Ltd. (Korea). The cesium solution used in the experiment was purchased from Kanto Chemical Corporation Inc. (Japan), a Cs^{133} standard solution (1000 mg/L), which is an isotope with similar chemical properties (Basu et al., 2018). Deionized water was used to prepare all solutions.

2.2. Preparation of CF-AA-PB

2.2.1. CF surface modification by AA

A schematic diagram of the CF surface modification method is shown in Fig. 1. The CF modification by AA is a type of radical polymerization. Free radicals on the CF backbone can be formed by the chemical initiator. The free radicals thus formed can add to monomers to form a covalent bond between the monomer and the CF. The propagation of the branch continues until termination occurs (Roy et al., 2009). In this study, we used potassium persulfate (KPS) as an initiator. The hydroxyl group of PVA as then reacted with the initiator to form a radical state. The acrylic acid monomer is then grafted on the radical site of CF.

A polymer solution was prepared using 60 mg of KPS and 2 mL of acrylic acid solution dispersed into 20 mL of deionized water in a vessel. Afterward, a cellulose filter ($20 \times 20\ cm^2$) was placed on a glass plate ($23 \times 23\ cm^2$), and the polymer solution was poured on a cellulose filter. The cellulose filter was then covered by a glass plate and the reaction proceeded in a dry oven filled with nitrogen gas to maintain anoxic conditions at 60 °C for 7 h. After the reaction ended, the CF-AA was washed with a mixed solution including a ratio 1:1 of ethanol and deionized water until the solution became transparent. The surface modified material was called CF-AA.

2.2.2. PB immobilization

PB immobilization on modified CF (CF-AA) and unmodified CF (CF) was performed via layer-by-layer (LBL) assembly, which is basically similar to in-situ synthesis methodology (Fig. 2). In-situ PB synthesis was performed by injecting the precursor of PB in series in the presence of the supporting materials. The major chemical reaction is given as Eq. 1 (Samain et al., 2013).

$$4FeCl_3 + 3K_4[Fe(CN)_6] \rightarrow Fe_4[Fe(CN)_6]_3 + 12KCl \quad (1)$$

250 mg of CF and CF-AA was added to a 50 mL solution of 20 mM $FeCl_3$ for 24 h. The supporting materials with immobilized iron(III) were then separated from the solution, and the product was reacted with 50 mL of 20 mM $K_4Fe(CN)_6$ solution for 15 min. PB growth via LBL assembly has an additional step of adding 50 mL of 5 mM $FeCl_3$ solution for 5 min after the previous two-step reaction has finished. The prepared materials are denoted as CF-PB and CF-AA-PB. The detailed advantages of LBL assembly compared to common in-situ PB synthesis was reported in our previous study (Wi et al., in press). The LBL assembly could significantly decrease PB leaching during washing.

2.2.3. Evaluation of PB elution

Afterward, the obtained product was dried at 60 °C for 48 h and washed five times in 50 mL of distilled water to evaluate the stability of the immobilized PB. After the washing experiment, the water was

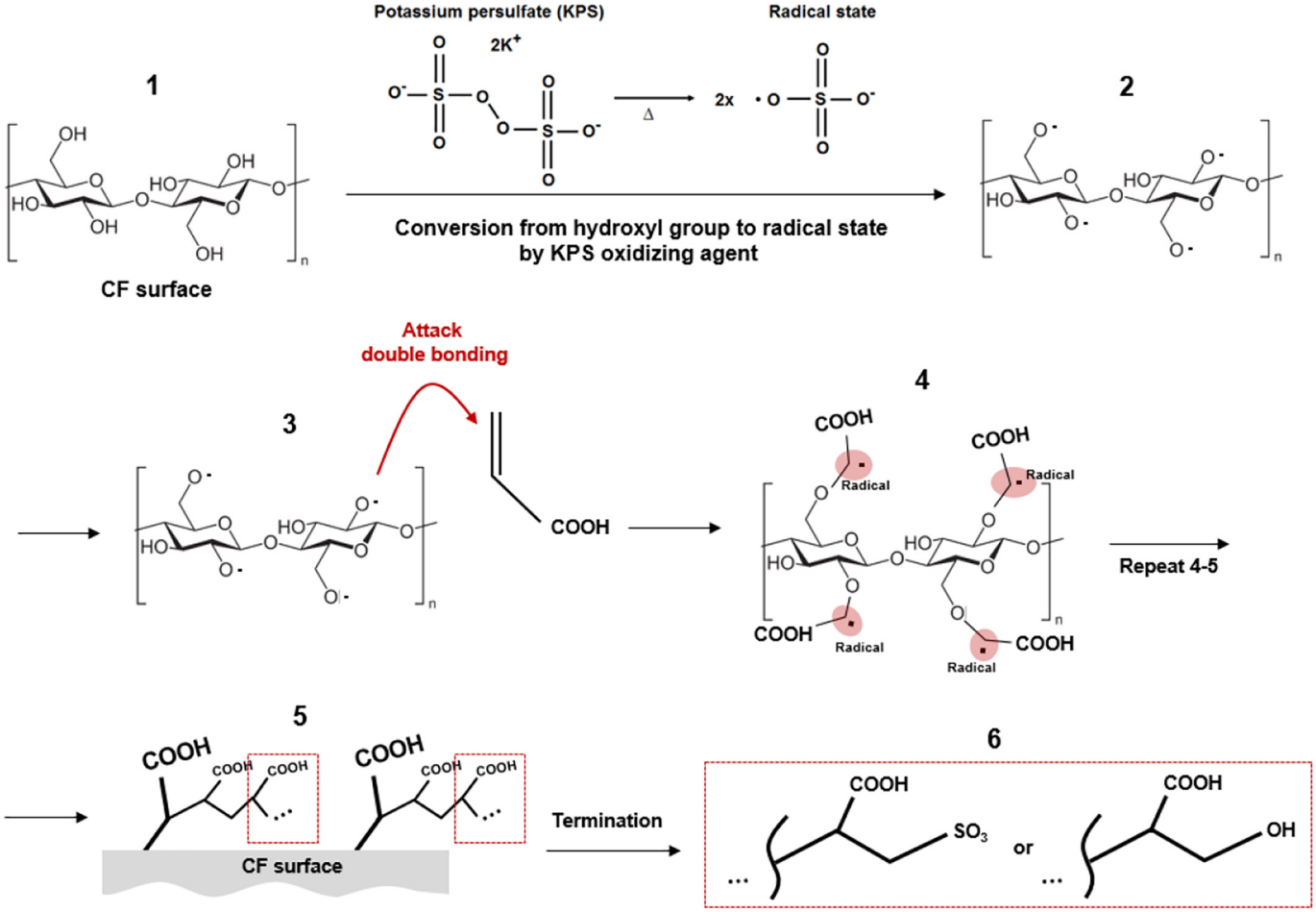

Fig. 1. Schematic of the surface modification method of cellulose filter using acrylic acid.

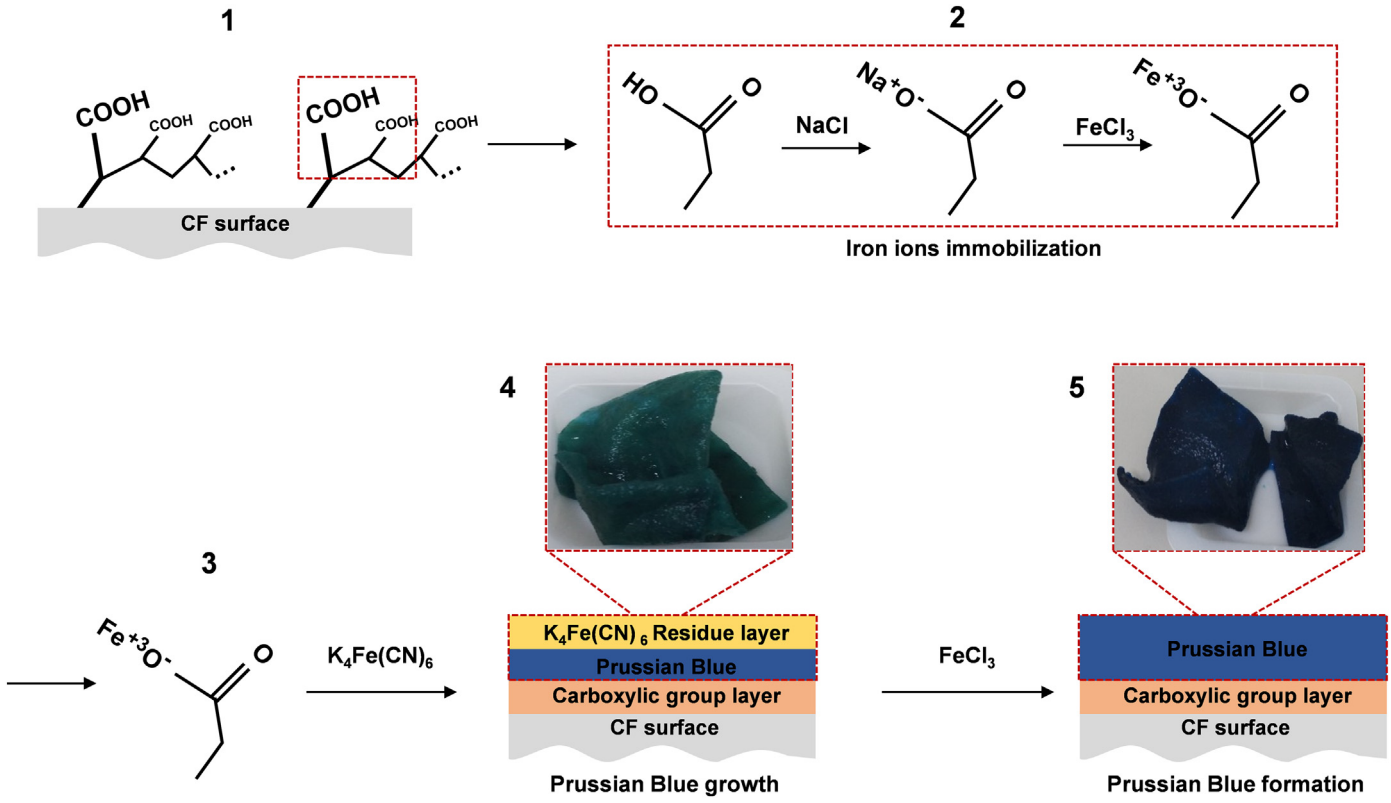

Fig. 2. Schematic of Prussian blue synthesis method for modified CF.

analyzed for PB at 690 nm using UV–Visible spectroscopy (UV–Vis, Libra S22, Biochrom).

2.3. Materials characterization

The effect of functionalization was evaluated by monitoring the changes in the functional groups on the surface of the PVA-PBs using Fourier-transform infrared spectroscopy (FTIR, TENSOR27, and Bruker, Germany) recorded in the 400–4000 cm^{-1} region. A scanning electron microscope with energy dispersed spectroscopy (SEM/EDS, JSM-6700F, JEOL, and Japan) was used to visualize surface modifications as well as to analyze the chemical composition qualitatively. Thermogravimetric analysis was also conducted to obtain information regarding thermal decomposition of the PBA-PBs as well as their chemical composition. Thermograms of the sample were recorded in the temperature range of 30–1000 °C with a heating rate of 10 °C/min in a nitrogen atmosphere, with a thermogravimetric analyzer (TGA, TG-DTA, Bruker, Germany).

2.4. Cesium adsorption experiments

2.4.1. Adsorption isotherms and kinetics

Adsorption isotherm testing was performed to evaluate the overall cesium adsorption capacity of CF-AA-PB together with CF-PB as a test control. 100 mg of the CF-PBs was mixed with 50 mL of cesium aqueous solutions with different initial concentrations ranging from 0.2 to 100 mg/L in a sealed conical polyethylene (PE) tube. The pH of the cesium aqueous solution was not adjusted and the solution was continuously shaken at 303 K for 24 h in an agitator. The cesium ion concentration in the supernatant was measured with an ICP-mass spectrometer (ICP-MS, NexION 350D, Perkin-Elmer, USA).

The sorption isotherm of the adsorbed cesium ion at equilibrium (q_e) was calculated using the Langmuir isotherm (Eq. 2) and Freundlich isotherm (Eq. 3) equations (Foo and Hameed, 2010). The Langmuir isotherm assumes that adsorption occurs at specific homogeneous sites on the surface of the adsorbent while The Freundlich equation based on sorption on a heterogeneous surface

$$q_e = \frac{q_m a_L C_e}{1 + a_L C_e} \tag{2}$$

$$q_e = K_F C_e^{\frac{1}{n}} \tag{3}$$

where q_e is the quantity of adsorbate adsorbed per unit weight of solid adsorbent, q_m is the maximum sorption capacity of the adsorbent (mg/g), C_e is the equilibrium concentration of the adsorbate in solution (mg/L), and a_L is the Langmuir affinity constant. K_F and 1/n are constants indicating the adsorption capacity and the adsorption intensity.

The adsorption kinetics of CF-PBs (CF-PB and CF-AA-PB) were investigated in a 10 mg/L Cs solution, similar to the isotherm test, except that several samples were taken at given time intervals (5 min, 10 min, 30 min, 1 h, 3 h, 10 h, and 24 h). The adsorption results were then fitted using the pseudo-first-order kinetic model (Eq. 4) and pseudo-second-order kinetic model (Eq. 5) (Ko et al., 2017).

$$q_t = q_e\left(1 - e^{-k_1 t}\right) \tag{4}$$

$$q_t = \frac{k_2 q_e^2 t}{1 + k_2 q_e t} \tag{5}$$

where q_t is the adsorbed amount at time t (mg/g), q_e is the equilibrium concentration (mg/g), k_1 is the first-order rate constant (1/min), and k_2 is the second-order rate constant (g/mg·min).

2.4.2. Effect of initial pH and water matrix

The effect of the initial pH was investigated using a 10 mg/L cesium solution at different initial pH of 4, 6, 8, and 10. pH was controlled by adding 1 M HCl and NaOH solution. The effect of the water matrix on cesium adsorption was investigated using two types of synthetic stream waters, soft and hard water, as suggested in the literature (Smith et al., 2002). The adsorption experiment was carried out with deionized water, soft water, and hard water with Cs initial concentration of 0.2, 0.5, 2, 5, 10, 20 mg/L and 24 h stirring. In all cases, 100 mg of adsorbent was applied. The water quality according to the raw water is shown in Table S1.

2.4.3. Filtration test

Continuous filtration experiments were conducted to simulate the situation where the cesium solution passed through the cellulose filter (Fig. 3). The size of the filtration unit was 7 cm × 10 cm × 1.5 cm, and the effective filtration area was 4 cm × 7 cm size. CF-AA-PB was placed in the filtration unit, and then 40 μg/L concentration cesium solution was introduced through the filter in the upward direction. The filtration velocity was maintained at 2 cm/min, and therefore the contact time was around 3 s. In order to simulate the situation where several filters are used in series or thicker filters are used, the filtrate was then returned into the raw water flask. Hydraulic retention time was calculated by the ratio between the total solution volume and the flow rate. Samples were taken at every hydraulic retention time until 15 cycles. In this experiment, cesium solutions prepared by spiking a cesium standard solution in deionized water and real stream water taken from the Han-ryu River were used to simulate actual conditions. Table S1 shows the results of the water quality analysis of real stream water.

3. Results and discussion

3.1. Material characterizations

3.1.1. Fourier transform infrared spectroscopy (FTIR)

The change in functional groups by AA treatment and PB immobilization was investigated using FTIR spectra shown in Fig. 4. First, the Pure CF presents peaks at 3640–3200 cm^{-1} (O—H), 3000–2850 cm^{-1} (C—H), and 1320–1000 cm^{-1} (C—O) according to the chemical composition of cellulose itself (Ciolacu et al., 2011). After the surface modification, C═O stretching of carboxyl groups was observed at 1760–1690 cm^{-1} (C═O, carboxylic acid). The spectra of the hydroxyl groups became weaker compared to the Pure CF. These results clearly show that the hydroxyl groups in Pure CF were converted to carboxyl groups by the AA. Once PB was formed on the CF or CF-AA, a strong peak at 2070 cm^{-1} (C≡N) was observed in the CF-PB and CF-AA-PB, which indicates the successful formation of PB (Kulesza et al., 1996).

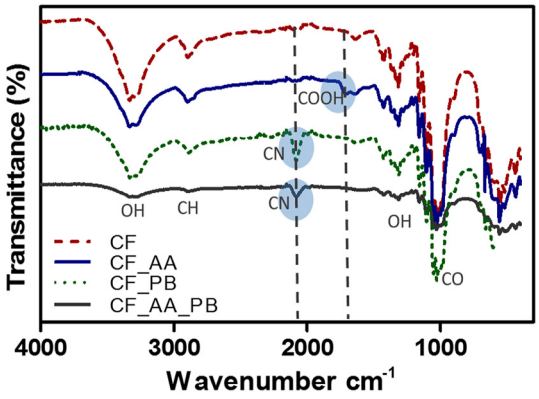

Fig. 4. FTIR spectra of CF, CF-AA, CF-PB, CF-AA-PB.

3.1.2. Scanning Electron microscope-energy dispersive spectroscopy (SEM-EDS)

Surface images of CF, CF-AA, CF-PB, and CF-AA-PB, which are magnified 1000 times through SEM, are shown in Fig. S1. The elemental composition was further analyzed by EDS as shown in Fig. S2 and Table 1. Overall, the CF has a structure in which thin fibers are entangled and with many internal spaces. The diameter of the fibers is approximately 10–20 μm. The CF-AA is very similar to CF except for a small deposit of NaCl, which was used during AA treatment. After synthesis of PB, particulate matter was easily identified from the surface of CF fibers and this was more obvious in the case of CF-AA-PB. The major element of this matter was iron and nitrogen, and therefore it can be confirmed as PB (Ishizaki et al., 2013).

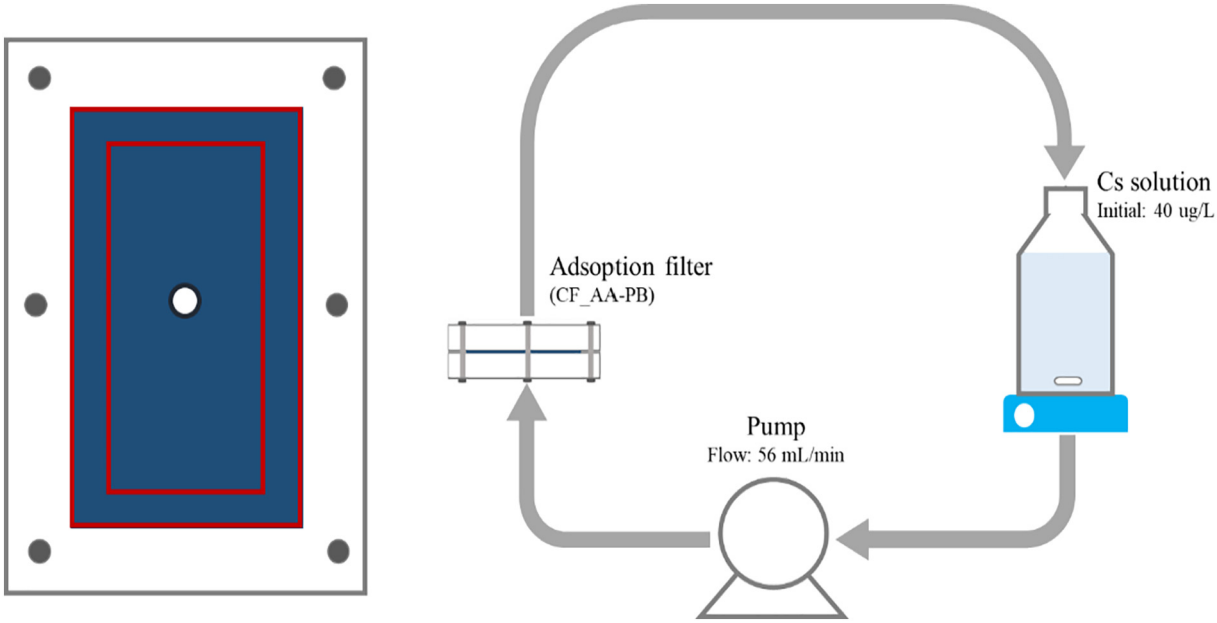

Fig. 3. Schematic of filtration test device.

Table 1
Weight percentages of elements on the surfaces of CF, CF-AA, CF-PB and CF-AA-PB (Unit: weight %).

Element type	C	O	N	Na	Cl	Fe
CF	33.20	66.80	–	–	–	–
CF-AA	32.22	55.64	–	4.18	7.97	–
CF-PB	29.65	55.34	9.14	–	–	5.87
CF-AA-PB	29.95	52.98	8.05	–	–	9.02

When the amount of iron attached through SEM-EDS was evaluated as a whole weight ratio, the CF-PB and CF_AA_PB had 5.87% and 9.02% iron, respectively, which indicates the effect of surface functionalization by AA on PB immobilization.

3.1.3. Thermogravimetric analysis (TGA)

The amount of PB immobilized on the synthetic material before and after modification by TGA was quantified and the results are shown in Fig. 5. The pristine CF was mostly decomposed at 330 °C–370 °C. The cellulose filter having a chemical formula of $(C_6H_{10}O_5)_n$ decomposes into carbon dioxide and water as the temperature rises. After CF decomposition in this temperature region, almost no weight remained, which indicates this sample contained pure CF.

CF-PB and CF-AA-PB showed decomposition of CF in the same temperature region. The early decomposition of CF-AA-PB was due to the decomposition of AA. However, a significant difference was observed after CF decomposition at 330–370 °C. More than 25% of the weight still remained at 370 °C, and this quantity further decreased as the temperature increased. The remaining weight could be immobilized PB, and the decrease in weight at high temperature can be explained as the degradation of PB particles, as reported in a previous study. It was reported that PB particles could be degraded through a collapse of bonding between Fe (II, III) iron and cyanide groups, by converting C≡N into N_2O and CO_2 (Jang et al., 2015). The remaining weight at 1000 °C for CF-PB and CF-AA-PB was 14.6% and 22.8%, respectively. Prussian blue is finally decomposed into Fe_2O_3, NO_2, and CO_2 as the temperature rises. Based on the remaining amount after decomposition, the Fe contents for CF-PB and CF-AA-PB were calculated to be 10.2% and 15.9%. This is similar to the previous SEM-EDS results. Finally, PB contents were calculated from the molecular composition. The amount of PB immobilized on the two materials was 26% for CF-PB and 40.7% for CF-AA-PB.

3.1.4. PB stability during washing

Fig. 6 shows the variation of PB concentration in the washing solution when the CF-PB and CF-AA-PB were washed by deionized water. Overall, the PB concentration in the washing solution was higher in CF-PB, which was not surface modified by AA. The maximum PB leaching was observed in the third time of washing as 3.15 μM. This result verified the advantage of using AA modification to enhance the stability of PB immobilization.

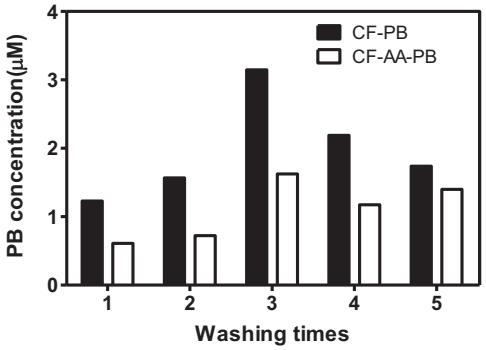

Fig. 6. Amount of desorbed PB after 5 washing of CF-PB and CF-AA-PB.

The amount of detached PB was further calculated based on the measured concentration and volume of water used for washing. The PB amount found in the washing water of CF-PB and CF-AA-PB was 0.423 mg and 0.237 mg, respectively. Using PB contents in CF-PB and CF-AA-PB obtained by TGA analysis (Section 3.1.3), the portion of detached PB was further calculated. The detached portion was 0.237 mg for CF-AA-PB, which can be calculated as 0.23% of PB immobilized. In the same manner, PB detachment from CF-PB was 0.65%. Based on this calculation, it can be determined that unmodified CF-PB loses 2.83 times more PB than AA modified CF-AA-PB. PB weakly bound to the -OH group of CF appeared to be separated by the force of washing. In the case of CF-AA-PB, the PB attached to the strong -COOH group is

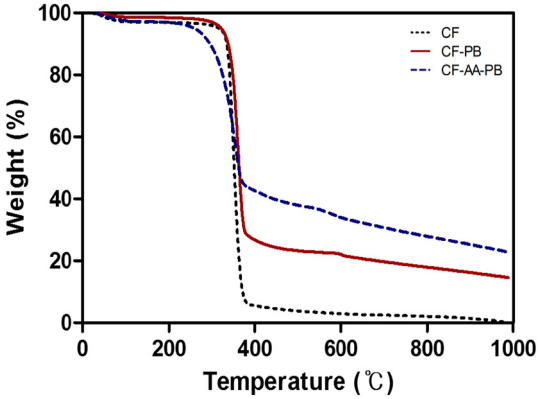

Fig. 5. TGA results of CF, CF-PB, CF-AA-PB.

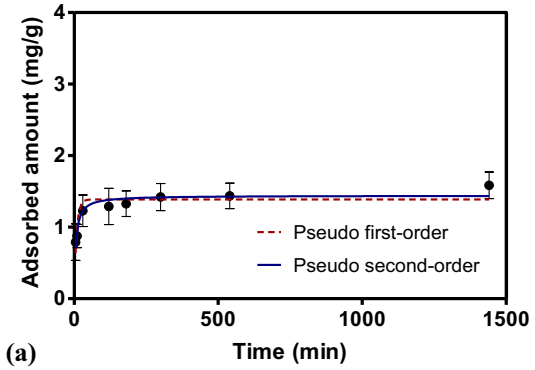

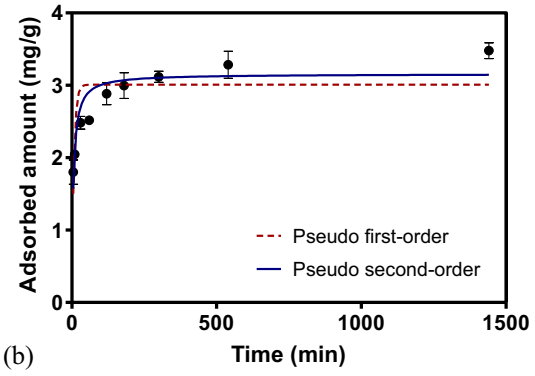

Fig. 7. Kinetics experiment of cesium adsorption of (a) CF-PB and (b) CF-AA-PB fitted by pseudo-first-order kinetic model and pseudo-second-order kinetic model.

strongly fixed and appears to have a small desorption amount. Therefore, it is concluded that AA treatment provides stable PB immobilization with less detachment.

3.2. Adsorption study of CF-AA-PB

3.2.1. Kinetic experiment

An adsorption kinetic experiment was conducted to determine the equilibrium time between CF-PBs and the cesium solution. Fig. 7 presents the adsorption capacities of CF-PB and CF-AA-PB with respect to time. The adsorption data were fitted by pseudo-first-order kinetics (Eq. (4)) and pseudo-second-order kinetics (Eq. (5)). The obtained kinetic parameters are given in Table S2.

The adsorbed cesium increased rapidly in the first 3 h, and then it was almost completely stabilized at 24 h. Between the two kinetic models that were applied, the pseudo-second-order kinetic fits better than the pseudo-first-order kinetic. This indicates that the cesium adsorption process is the chemical interactions between the functional groups of adsorbent and cesium ions, and this is in good agreement with previous reports on cesium adsorption by PB (Jang and Lee, 2016). The pseudo-second-order kinetic constants for CF-PB and CF-AA-PB were 0.08733 and 0.06283 g/mg·min, respectively. It appears that the unmodified CF-PB has relatively higher kinetic constants, which indicates slight pore blockage of the CF filter by AA modification. However, the difference was not significant enough to hinder overall adsorption.

The pseudo-first-order and pseudo-second-order kinetic constants of CF-AA-PB were 0.1384 min^{-1} and 0.06283 $g \cdot mg^{-1} \cdot min^{-1}$, respectively, which is comparable to or even higher than previous reports (Basu et al., 2018; Jang and Lee, 2016; Yang et al., 2018), and these high values are due to faster mass transfer by the very porous nature of CF filter. Since the adsorption equilibrium could be achieved after 3 to 6 h of adsorption time, we used 24 h of adsorption time for further equilibrium experiments.

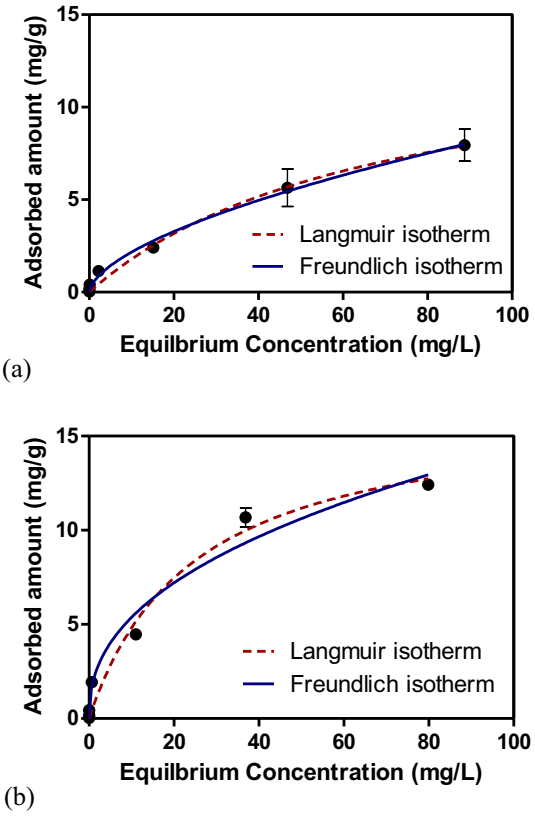

Fig. 8. Adsorption isotherm experiment of cesium of (a) CF-PB and (b) CF-AA-PB fitted by Langmuir isotherm and Freundlich isotherm.

3.2.2. Adsorption isotherm experiment

Adsorption isotherm experiments were conducted to compare the cesium adsorption capacities of CF-PB and CF-AA-PB, and the results were fitted with Langmuir adsorption and Freundlich adsorption, as shown in Fig. 8 and Table S3. A control experiment with Pure-CF and CF-AA was also conducted in parallel (Fig. S3). The Pure-CF and CF-AA did not show any cesium adsorption while CF-PB and CF-AA-PB showed cesium adsorption capabilities. This indicates that the cesium adsorption ability of the prepared CF-PBs is due to the addition of PB, not the supporting material or surface modification, CF or AA.

When the cesium adsorption capacities of CF-PB and CF-AA-PB were compared, CF-AA-PB showed much higher cesium adsorption capacity compared to CF-PB. For example, the maximum cesium adsorption obtained by the experiments was 7.95 and 12.42 mg/g for CF-PB and CF-AA-PB, respectively, when the initial cesium concentration was 100 mg/L. The cesium adsorption capacity was increased by around 56% by surface modification. This increased adsorption capacity (56%) was exactly identical as increased PB contents (26% to 40.7%; 56.5% increase). Therefore, we can conclude that the cesium adsorption capacity was increased by increased PB content. When the adsorption affinity values (a_L) were compared, CF-PB was 0.01457 L/mg, CF-AA-PB was 0.04059 L/mg, and CF-AA-PB had higher cesium adsorption affinity, indicating that the adsorbed affinity of the modified material was higher.

The obtained adsorption capacity value (q_m) is compared with the previously reported values in Table S4. PB itself showed very high cesium adsorption capacities in a few hundred mg/L range. However, the composite materials containing PB showed much low q_m value due to the low PB contents. Especially, PB based composites in bead or sponge or filter shape have low q_m value compared to powder shape adsorbent due to inhibition in mass transfer. For example, bead or sponge foam of adsorbent showed much low q_m value in the range of 0.154–43.5 mg/L. The result obtained from our study is in the range of q_m value for structured adsorbents containing PB. Moreover, the testing concentration range also affects q_m value. Generally, testing in a high concentration range gives a higher q_m value. We used a 100 mg/L as a maximum cesium concentration during isotherm test, which is generally accepted a range of testing.

It has been commonly accepted that cesium adsorption on PB was driven by both of physisorption and chemisorption. Ishizaki et al. (2013) explained that the exclusive abilities of PB to adsorb hydrated cesium ions are caused by regular lattice spaces surrounded by cyanide-bridged metals. On the other hand, chemisorption was also considered for cesium adsorption by PB. A common PB with a formula of $Fe_4[Fe(CN)_6]_3 \cdot xH_2O$ have many defect sites (vacant spaces) of $[Fe(CN)_6]^{4-}$ filled with coordination and crystallization water molecules due to a high value of the number of waters of crystallization. The similar approach and explanation could be found in the literature (Vipin et al., 2013). The adsorption data were fitted with Langmuir isotherm as well as Freundlich isotherm in order to distinguish dominant adsorption isotherm, however, the R^2 value for both model are similar while Langmuir isotherm has slightly higher R^2 value. Therefore, we can conclude that physisorption and chemisorption can occur simultaneously in our test condition.

3.2.3. Effect of initial pH

Effect of pH on the metal adsorption is greatly important since the solution pH affects both the binding sites and the metal speciation. In this study, the influence of pH on cesium adsorption was investigated by changing the initial pH between 4 and 10. Fig. 9 (a) presents the initial pH and final pH after 24 h of adsorption experiments as well as the amount of adsorbed cesium for each pH condition. The final pH was lower in all cases, and the pH decrease was more significant when the initial pH was high. For example, when the initial pH was adjusted to

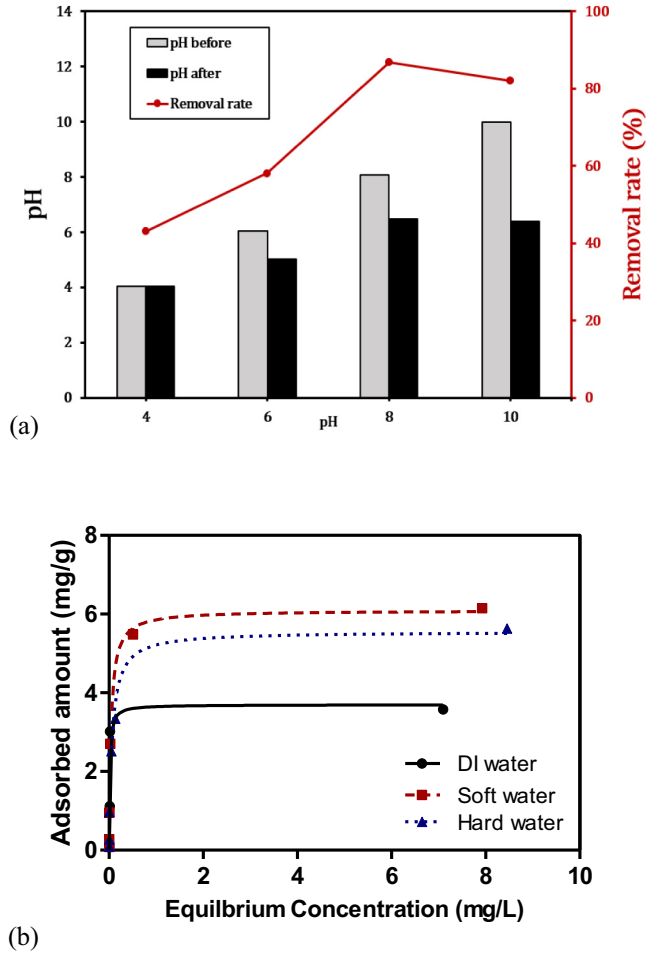

Fig. 9. (a) Cesium adsorption of CF-AA-PB in range of pH 4–10 and pH change during the adsorption experiment (b) Effect of water matrix on cesium adsorption by CF-AA-PB.

10, it decreased to 6.2 after 24 h. The decrease in pH could be explained by the following Eq. (6) (Ishizaki et al., 2013):

$$Fe^3-OH_2 + Cs^+A^- \rightarrow Fe^3-OH^-Cs^+ + H^+A^- \quad (6)$$

The initial and final pH was closely linked to cesium ion adsorption capacity. Higher cesium adsorption capacity was obtained in weak alkaline conditions. When the pH was increased from pH 6 to pH 8, the increase in treatment efficiency by CF-AA-PB was as high as about 20%. The maximum removal efficiency of CF-AA-PB was 86.79% at pH 8. The lower performance under acidic conditions resulted from competition between protons (H^+) and cesium (Cs^+), resulting in low adsorption capacity, as reported earlier (Feng et al., 2016; Yang et al., 2018). The influence of pH is high in the case of ion-exchange processes, especially for monovalent cations because of the ion-exchange competition. At low pH, ion exchange sites are mainly protonated, making them less available for cation. When pH values increase, the sites become available for cation, leading to higher adsorption. (Vipin et al., 2013)

3.2.4. Effect of water matrix

The effect of the water matrix was investigated to evaluate the practical feasibility of the system when exposed to environmental media containing interfering substances. We used three types of water matrix for this study, deionized water, soft water, and hard water. Soft and hard water are synthetic water matrices used to represent common surface water and groundwater. Both synthetic waters contained various cations including Ca^{2+}, Na^+, and K^+, which can be competitors with Cs^+ because they can be exchanged in the PB lattice structure. In this study, an adsorption isotherm test in a low concentration range (~20 mg/L) was performed for the three water matrixes, and the results were fitted with the Langmuir model, as shown in Fig. 9(b).

The maximum cesium adsorption obtained by the Langmuir isotherm was 4.437 mg/g for deionized water, 6.094 mg/g for soft water, and 5.556 mg/g for hard water. The maximum adsorption amount of soft water and hard water was higher than that of deionized water. It is very interesting that adsorption capacity was not decreased even when competing cations were present in the water matrix. These results should be carefully discussed in relation to the pH change observed during adsorption. The final pH of deionized water was 4.64 while that of soft water and hard water was around 7.7. As described earlier, pH was decreased by H^+ ions excreted into the solution during cesium adsorption via ion exchange, and lower pH is not favorable for further cesium adsorption. Soft water and hard water contain alkalinity (385 and 2010 μeq/L, respectively), and therefore the pH change was minimized.

When the adsorption pH is similar between soft-water and hard-water, competition among cations plays a role to determine the cesium adsorption performance. Soft water showed better cesium adsorption performance compared to hard water even though the adsorption pH was similar. This might be due to the high concentration of cations in hard water. The sum of cations in hard water was 4.04 mM, while it was 0.93 mM for soft water, and therefore more than four times more cations were competing with cesium for adsorption. It was reported that cesium adsorption was negatively affected by the high ionic condition (Sangvanich et al., 2010). This competitive adsorption is directly related to the adsorption affinity obtained by Langmuir adsorption. Adsorption affinities were calculated as 51.09 L/mg for deionized water, 24.33 L/mg for soft water, and 15.4 L/mg for hard water.

3.3. Continuous adsorption experiment

A continuous filtration test was conducted to demonstrate the feasibility of CF-AA-PB as a cesium adsorbent for a water treatment system.

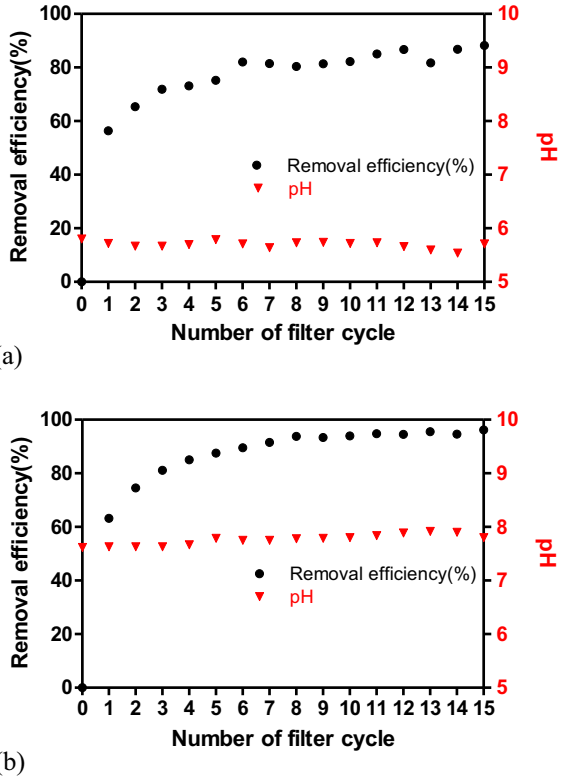

Fig. 10. Continuous operation experiment using CF-AA-PB (a) deionized water, (b) real stream water.

The filtration system was constructed with a single layer of CF-AA-PB (7 cm × 4 cm) and a solution of 40 μg/L cesium was added into the filtration unit at a filtration velocity of 2 cm/min. In this experiment, we tested two different water matrixes, deionized water, and actual stream water, in order to simulate the actual treatment process, and the results are shown in Fig. 10. The sum of cations in actual stream water was 3.7 mM, which is close to the case of hard water tested in Section 3.2.4. Overall alkalinity (1.30 meq/L) was in the range of soft water (0.39 meq/L) and hard water (2.01 meq/L), therefore, stable pH during cesium adsorption experiments could be expected.

The cesium removal efficiency was 56.3% at the first cycle in deionized water, and the removal efficiency was increased to 75.2% at 5 cycles, 82.2% at 10 cycles, and 88.2% at 15 cycles. The initial pH of deionized water was 5.8 and there was little change in pH during the treatment.

When applied to actual stream water, the treatment efficiency was higher than that of deionized water because of the pH effect. The initial pH of the initial stream water was 7.62 and a change of pH was not observed due to the presence of alkalinity. The cesium removal efficiency was 63.2% at the first cycle in deionized water, and the treatment efficiency was increased to 87.6% at 5 cycles, 94% at 10 cycles, and 96.3% at 15 cycles. Comparing the treatment efficiency according to the water matrix, the removal efficiency in stream water was approximately 10% higher than that of deionized water. This result is very promising for water treatment because the removal efficiency was not inhibited by the water matrix. The developed filter can be easily installed at the water intake with a few centimeter thicknesses to prevent contaminated water intake.

4. Conclusion

The goal of this study was to develop a method of preparing a filter type cesium adsorbent containing PB as the active adsorption material. A cellulose filter was functionalized by reaction with acrylic acid to convert –OH functional groups to –COOH to enhance the immobilization and stability of the PB. The effect of functionalization on PB immobilization was demonstrated by washing experiments and FTIR and SEM-EDS analyses. The adsorption kinetics and isotherms of the CF-AA-PB were further investigated. The adsorption occurred rapidly during the initial 30 min and the adsorption rates of CF-PB and CF-AA-PB were not significantly different. The maximum adsorption capacity and the adsorption affinity were enhanced by surface modification. The adsorption behavior was sensitive to the initial pH and buffering. The best cesium adsorption performance was obtained at an alkaline pH range and the adsorption capacity was not significantly hindered by the water matrix. Finally, the prepared CF-AA-PB was used as a filter for continuous adsorption testing. From the results of the continuous filtration test, the CF-AA-PB showed 96.3% cesium removal efficiency when actual stream water was used. Based on the above results, the CF-AA-PB prepared in this study demonstrated the potential for practical application as a filter-type adsorbent for the remediation of radioactive cesium.

Acknowledgments

This study was supported by the Creative Convergence Research Project (CAP-15-07-KICT) of the National Research Council of Science and Technology (NST).

Appendix A. Supplementary data

Supplementary data to this article can be found online at https://doi.org/10.1016/j.scitotenv.2019.03.234.

References

Alamudy, H.A., Cho, K., 2018. Selective adsorption of cesium from an aqueous solution by a montmorillonite-Prussian blue hybrid. Chem. Eng. J. 349, 595–602. https://doi.org/10.1016/j.cej.2018.05.137.

Ali, I., AL-Hammadi, S.A., Saleh, T.A., 2018. Simultaneous sorption of dyes and toxic metals from waters using synthesized titania-incorporated polyamide. J. Mol. Liq. 269, 564–571. https://doi.org/10.1016/j.molliq.2018.08.081.

Aoyama, M., Hirose, K., 2004. Artificial radionuclides database in the Pacific Ocean: HAM database. Sci. World J. 4, 200–215. https://doi.org/10.1100/tsw.2004.15.

Awual, M.R., Yaita, T., Taguchi, T., Shiwaku, H., Suzuki, S., Okamoto, Y., 2014. Selective cesium removal from radioactive liquid waste by crown ether immobilized new class conjugate adsorbent. J. Hazard. Mater. 278, 227–235. https://doi.org/10.1016/j.jhazmat.2014.06.011.

Basu, H., Saha, S., Pimple, M.V., Singhal, R.K., 2018. Graphene-Prussian blue nanocomposite impregnated in alginate for efficient removal of cesium from aquatic environment. J. Environ. Chem. Eng. 6, 4399–4407. https://doi.org/10.1016/j.jece.2018.06.062.

Buesseler, K.O., Jayne, S.R., Fisher, N.S., Rypina, I.I., Baumann, H., Baumann, Z., Breier, C.F., Douglass, E.M., George, J., Macdonald, A.M., Miyamoto, H., Nishikawa, J., Pike, S.M., Yoshida, S., 2012. Fukushima-derived radionuclides in the ocean and biota off Japan. Proc. Natl. Acad. Sci. U. S. A. 109, 5984–5988. https://doi.org/10.1073/pnas.1120794109.

Chen, F., Jin, G., Peng, S., Liu, X., Tian, J., 2016. Recovery of cesium from residual salt lake brine in Qarham playa of Qaidam Basin with Prussian blue functionalized graphene/carbon fibers composite. Colloids Surf. A Physicochem. Eng. Asp. 509, 359–366. https://doi.org/10.1016/j.colsurfa.2016.09.030.

Ciolacu, D., Ciolacu, F., Popa, V.I., 2011. Amorphous cellulose—structure and characterization. Cellul. Chem. Technol. 45, 13–21.

Delchet, C., Tokarev, A., Dumail, X., Toquer, G., Barré, Y., Guari, Y., Guerin, C., Larionova, J., Grandjean, A., 2012. Extraction of radioactive cesium using innovative functionalized porous materials. RSC Adv. 2, 5707–5716. https://doi.org/10.1039/C2RA00012A.

Dresselhaus, M., Thomas, I., 2001. Alternative energy technologies. Nature. 414, 332–337. https://doi.org/10.1038/35104599.

El-Kamash, A., 2008. Evaluation of zeolite A for the sorptive removal of Cs and Sr_2 ions from aqueous solutions using batch and fixed bed column operations. J. Hazard. Mater. 151, 432–445. https://doi.org/10.1016/j.jhazmat.2007.06.009.

Faustino, P.J., Yang, Y., Progar, J.J., Brownell, C.R., Sadrieh, N., May, J.C., Leutzinger, E., Place, D.A., Duffy, E.P., Houn, F., Loewke, S.A., Mecozzi, V.J., Ellison, C.D., Khan, M.A., Hussain, A.S., Lyon, R.C., 2008. Quantitative determination of cesium binding to ferric hexacyanoferrate: Prussian blue. J. Pharm. Biomed. Anal. 47, 114–125. https://doi.org/10.1016/j.jpba.2007.11.049.

Feng, S., Li, X., Ma, F., Liu, R., Fu, G., Xing, S., Yue, X., 2016. Prussian blue functionalized microcapsules for effective removal of cesium in a water environment. RSC Adv. 6, 34399–34410. https://doi.org/10.1039/C6RA01450J.

Foo, K.Y., Hameed, B.H., 2010. Insights into the modeling of adsorption isotherm systems. Chem. Eng. J. 156, 2–10. https://doi.org/10.1016/j.cej.2009.09.013.

Forsberg, C.W., 2009. Sustainability by combining nuclear, fossil, and renewable energy sources. Prog. Nucl. Energy 51, 192–200. https://doi.org/10.1016/j.pnucene.2008.04.002.

Ge, H., Wang, J., 2017. Ear-like poly (acrylic acid)-activated carbon nanocomposite: a highly efficient adsorbent for removal of Cd (II) from aqueous solutions. Chemosphere. 169, 443–449. https://doi.org/10.1016/j.chemosphere.2016.11.069.

Haas, P.A., 1993. A review of information on ferrocyanide solids for removal of cesium from solutions. Sep. Sci. Technol. 28, 2479–2506. https://doi.org/10.1080/01496399308017493.

Honda, M.C., Aono, T., Aoyama, M., Hamajima, Y., Kawakami, H., Kitamura, M., Masumoto, Y., Miyazawa, Y., Takigawa, M., Saino, T., 2012. Dispersion of artificial caesium-134 and-137 in the western North Pacific one month after the Fukushima accident. Geochem. J. 46, e1–e9. https://doi.org/10.2343/geochemj.1.0152.

Hu, B., Fugetsu, B., Yu, H., Abe, Y., 2012. Prussian blue caged in spongiform adsorbents using diatomite and carbon nanotubes for elimination of cesium. J. Hazard. Mater. 217-218, 85–91. https://doi.org/10.1016/j.jhazmat.2012.02.071.

International Atomic Energy Agency/Power Reactor Information System, 2018. The database on nuclear power reactors. https://pris.iaea.org/pris/ (accessed 30 November 2018).

International Atomic Energy Agency, 2018b. Energy, electricity and nuclear power estimates for the period up to 2050. https://www.iaea.org/publications/11120/energy-electricity-and-nuclear-power-estimates-for-the-period-up-to-2050 (accessed 30 November 2018).

International Atomic Energy Agency, 2018c. Incident and Trafficking Database (ITDB). https://www.iaea.org/resources/databases/itdb (accessed 5 December 2018).

Ishizaki, M., Akiba, S., Ohtani, A., Hoshi, Y., Ono, K., Matsuba, M., Togashi, T., Kananizuka, K., Sakamoto, M., Takahashi, A., Kawamoto, T., Tanaka, H., Watanabe, M., Arisaka, M., Nankawa, T., Kurihara, M., 2013. Proton-exchange mechanism of specific Cs adsorption via lattice defect sites of Prussian blue filled with coordination and crystallization water molecules. Dalton Trans. 42, 16049–16055. https://doi.org/10.1039/C3DT51637G.

Jang, J., Lee, D.S., 2016. Magnetic Prussian blue nanocomposites for effective cesium removal from aqueous solution. Ind. Eng. Chem. Res. 5, 3852–3860. https://doi.org/10.1021/acs.iecr.6b00112.

Jang, S., Haldorai, Y., Lee, G., Hwang, S., Han, Y., Roh, C., Huh, Y.S., 2015. Porous three-dimensional graphene foam/Prussian blue composite for efficient removal of radioactive 137 Cs. Sci. Rep. 5, srep17510. https://doi.org/10.1038/srep17510.

Jia, F., Wang, J., 2017. Separation of cesium ions from aqueous solution by vacuum membrane distillation process. Prog. Nucl. Energy 98, 293–300. https://doi.org/10.1016/j.pnucene.2017.04.008.

Kadam, A.A., Jang, J., Lee, D.S., 2016. Facile synthesis of pectin-stabilized magnetic graphene oxide Prussian blue nanocomposites for selective cesium removal from aqueous solution. Bioresour. Technol. 216, 391–398. https://doi.org/10.1016/j.biortech.2016.05.103.

Kim, Y., Kim, I., Lee, T.S., Lee, E., Lee, K.J., 2018. Porous hydrogel containing Prussian blue nanoparticles for effective cesium ion adsorption in aqueous media. J. Ind. Eng. Chem. 60, 465–474. https://doi.org/10.1016/j.jiec.2017.11.034.

Kim, H., Kim, J., Oh, D., Hwang, Y., 2018a. Development of filter-type adsorbent containing Prussian blue for adsorption of cesium in aqueous phase. J. Korean. Soc. Environ. Eng. 40, 334–340. https://doi.org/10.4491/KSEE.2018.40.8.334.

Kim, H., Kim, M., Lee, W., Kim, S., 2018b. Rapid removal of radioactive cesium by polyacrylonitrile nanofibers containing Prussian blue. J. Hazard. Mater. 347, 106–113. https://doi.org/10.1016/j.jhazmat.2017.12.050.

Ko, D., Lee, J.S., Patel, H.A., Jakobsen, M.H., Hwang, Y., Yavuz, C.T., Hansen, H.C.B., Andersen, H.R., 2017. Selective removal of heavy metal ions by disulfide linked polymer networks. J. Hazard. Mater. 332, 140–148. https://doi.org/10.1016/j.jhazmat.2017.03.007.

Kong, B., Tang, J., Wu, Z., Wei, J., Wu, H., Wang, Y., Zheng, G., Zhao, D., 2014. Ultralight mesoporous magnetic frameworks by interfacial assembly of Prussian blue nanocubes. Angew. Chem. 53, 2888–2892. https://doi.org/10.1002/anie.201308625.

Kulesza, P.J., Malik, M.A., Denca, A., Strojek, J., 1996. In situ FT-IR/ATR spectroelectrochemistry of Prussian blue in the solid state. Anal. Chem. 68, 2442–2446. https://doi.org/10.1021/ac950380k.

Lai, Y., Chang, Y., Chen, M., Lo, Y., Lai, J., Lee, D., 2016. Poly(vinyl alcohol) and alginate cross-linked matrix with immobilized Prussian blue and ion exchange resin for cesium removal from waters. Bioresour. Technol. 214, 192–198. https://doi.org/10.1016/j.biortech.2016.04.096.

Loos-Neskovic, C., Ayrault, S., Badillo, V., Jimenez, B., Garnier, E., Fedoroff, M., Jones, D.J., Merinov, B., 2004. Structure of copper-potassium hexacyanoferrate (II) and sorption mechanisms of cesium. J. Solid State Chem. 177, 1817–1828. https://doi.org/10.1016/j.jssc.2004.01.018.

Ma, F., Li, Z., Zhao, H., Geng, Y., Zhou, W., Li, Q., Zhang, L., 2017. Potential application of graphene oxide membranes for removal of Cs (I) and Sr (II) from high level-liquid waste. Sep. Purif. Technol. 188, 523–529. https://doi.org/10.1016/j.seppur.2017.07.062.

Manolopoulou, M., Vagena, E., Stoulos, S., Ioannidou, A., Papastefanou, C., 2011. Radioiodine and radiocesium in Thessaloniki, Northern Greece due to the Fukushima nuclear accident. J. Environ. Radioact. 102, 796–797. https://doi.org/10.1016/j.jenvrad.2011.04.010.

Nightingale Jr., E.R., 1959. Phenomenological theory of ion solvation. Effective radii of hydrated ions. J. Phys. Chem. 63, 1381–1387. https://doi.org/10.1021/j150579a011.

Nuclear Regulation Authority Japan, 2018. Readings of radioactivity in drinking water by prefecture. http://www.nsr.go.jp/english/index.html, Accessed date: 30 November 2018.

Olatunji, M.A., Khandaker, M.U., Mahmud, H.E., Amin, Y.M., 2015. Influence of adsorption parameters on cesium uptake from aqueous solutions-a brief review. RSC Adv. 5, 71658–71683. https://doi.org/10.1039/C5RA10598F.

Pau, P.C.F., Berg, J., McMillan, W., 1990. Application of Stokes' law to ions in aqueous solution. J. Phys. Chem. 94, 2671–2679. https://doi.org/10.1021/j100369a080.

Qian, J., Han, X., Yang, S., Kuang, L., Hua, D., 2018. A strategy for effective cesium adsorption from aqueous solution by polypentacyanoferrate-grafted polypropylene fabric under γ-ray irradiation. J. Taiwan Inst. Chem. Eng. 89, 162–168. https://doi.org/10.1016/j.jtice.2018.04.036.

Roy, D., Semsarilar, M., Guthrie, J.T., Perrier, S., 2009. Cellulose modification by polymer grafting: a review. Chem. Soc. Rev. 38, 2046–2064. https://doi.org/10.1039/B808639G.

Saleh, T.A., Sarı, A., Tuzen, M., 2016. Chitosan-modified vermiculite for As (III) adsorption from aqueous solution: equilibrium, thermodynamic and kinetic studies. J. Mol. Liq. 219, 937–945. https://doi.org/10.1016/j.molliq.2016.03.060.

Samain, L., Grandjean, F., Long, G.J., Martinetto, P., Bordet, P., Strivay, D., 2013. Relationship between the synthesis of Prussian blue pigments, their color, physical properties, and their behavior in paint layers. J. Phys. Chem. C 117, 9693–9712. https://doi.org/10.1021/jp3111327.

Sangvanich, T., Sukwarotwat, V., Wiacek, R.J., Grudzien, R.M., Fryxell, G.E., Addleman, R.S., Timchalk, C., Yantasee, W., 2010. Selective capture of cesium and thallium from natural waters and simulated wastes with copper ferrocyanide functionalized mesoporous silica. J. Hazard. Mater. 182, 225–231. https://doi.org/10.1016/j.jhazmat.2010.06.019.

Smith, E., Davison, W., Hamilton-Taylor, J., 2002. Methods for preparing synthetic freshwaters. Water Res. 36, 1286–1296. https://doi.org/10.1016/S0043-1354(01)00341-4.

Smuleac, V., Bachas, L., Bhattacharyya, D., 2010. Aqueous - phase synthesis of PAA in PVDF membrane pores for nanoparticle synthesis and dichlorobiphenyl degradation. J. Membr. Sci. 346, 310–317. https://doi.org/10.1016/j.memsci.2009.09.052.

Tan, X., Fang, M., Tan, L., Liu, H., Ye, X., Hayat, T., Wang, X., 2018. Core–shell hierarchical C@$Na_2Ti_3O_7 \cdot 9H_2O$ nanostructures for the efficient removal of radionuclides. Environ. Sci.: Nano 5, 1140–1149. https://doi.org/10.1039/C8EN00149A.

Tka, N., Jabli, M., Saleh, T.A., Salman, G.A., 2018. Amines modified fibers obtained from natural Populus tremula and their rapid biosorption of acid blue 25. J. Mol. Liq. 250, 423–432. https://doi.org/10.1016/j.molliq.2017.12.026.

Turgis, R., Arrachart, G., Delchet, C., Rey, C., Barré, Y., Pellet-Rostaing, S., Guari, Y., Larionova, J., Grandjean, A., 2013. An original "click and bind" approach for immobilizing copper hexacyanoferrate nanoparticles on mesoporous silica. Chem. Mater. 25, 4447–4453. https://doi.org/10.1021/cm4029935.

Vipin, A.K., Hu, B., Fugetsu, B., 2013. Prussian blue caged in alginate/calcium beads as adsorbents for removal of cesium ions from contaminated water. J. Hazard. Mater. 258-259, 93–101. https://doi.org/10.1016/j.jhazmat.2013.04.024.

Wi, H., Kang, S.W., Hwang, Y., 2019. Immobilization of Prussian blue nanoparticles in acrylic acid-surface functionalized poly(vinyl alcohol) sponges for cesium adsorption. Environ. Eng. Res. 24 (1), 173–179. https://doi.org/10.4491/eer.2018.177.

Wi, H., Kim, H., Kang, S.W., Hwang, Y., 2019. Prussian blue immobilization on various filter materials through layer-by-layer assembly for effective cesium adsorption. Membr. Water. Treat. (in press).

Yang, H., Li, H., Zhai, J., Sun, L., Zhao, Y., Yu, H., 2014a. Magnetic Prussian blue/graphene oxide nanocomposites caged in calcium alginate microbeads for elimination of cesium ions from water and soil. Chem. Eng. J. 246, 10–19. https://doi.org/10.1016/j.cej.2014.02.060.

Yang, J., Wang, X., Zhu, M., Liu, H., Ma, J., 2014b. Investigation of PAA/PVDF-NZVI hybrids for metronidazole removal: synthesis, characterization, and reactivity characteristics. J. Hazard. Mater. 264, 269–277. https://doi.org/10.1016/j.jhazmat.2013.11.037.

Yang, H., Jang, S., Hong, S.B., Lee, K., Roh, C., Huh, Y.S., Seo, B.K., 2016. Prussian blue-functionalized magnetic nanoclusters for the removal of radioactive cesium from water. J. Alloys Compd. 657, 387–393. https://doi.org/10.1016/j.jallcom.2015.10.068.

Yang, H., Hwang, K.S., Park, C.W., Lee, K., 2017. Sodium-copper hexacyanoferrate-functionalized magnetic nanoclusters for the highly efficient magnetic removal of radioactive caesium from seawater. Water Res. 125, 81–90. https://doi.org/10.1016/j.watres.2017.08.037.

Yang, H., Hwang, J.R., Lee, D.Y., Kim, K.B., Park, C.W., Kim, H.R., Lee, K.W., 2018. Eco-friendly one-pot synthesis of Prussian blue-embedded magnetic hydrogel beads for the removal of cesium from water. Sci. Rep. 8, 11476. https://doi.org/10.1038/s41598-018-29767-y.

Yuan, L., Smith, A.C., 2015. Numerical modeling of water spray suppression of conveyor belt fires in a large-scale tunnel. Process. Saf. Environ. Prot. 95, 93–101. https://doi.org/10.1016/j.psep.2015.02.018.

Yuan, S., Feng, L., Wang, K., Pang, J., Bosch, M., Lollar, C., Sun, Y., Qin, J., Yang, X., Zhang, P., Wang, Q., Zou, L., Zhang, Y., Zhang, L., Fang, Y., Li, J., Zhou, H.-C., 2018. Stable metal–organic frameworks: design, synthesis, and applications. Adv. Mater. 30, 1704303. https://doi.org/10.1002/adma.201704303.